ERUPTIVE INSTABILITY OF MAGNETIC ARCADES*

B. VRŠNAK

Hvar Observatory, Hvar, Yugoslavia

Abstract. Eruptive prominences trace disruptions of magnetic arcades in which they are embedded. The stability of an arcade containing an electric current filament at its axis is discussed. The model provides criteria for the onset of the eruptive instability in terms of prominence twist and overall geometry, i.e., the parameters which could be measured directly. The evolution of the eruption is analyzed, and the dependence of the acceleration and the pitch of field-lines on the height is established. The model is compared with the observations of one eruptive prominence where the development of helical structure was followed.

1. Introduction

The Extreme UV Spectroheliograph on-board Skylab revealed that the structure of the solar corona above an active region could be described by a system of loops spanning over the magnetic inversion line and connecting the regions of opposite magnetic polarity. Such magnetic arcades exist also on a larger scale, interconnecting active regions. The footpoints of an arcade can extend several 10^5 km along the magnetic inversion line, while its height can reach more than 2×10^5 km (Sheeley *et al.*, 1975). The most powerful solar flares (two-ribbon flares) occur as a part of an arcade disruption (Švestka, 1989) which put the evolution and stability of such structures in the focus of numerous studies (Priest, 1982; Hood, 1988, and references given therein).

Frequently, condensations of cold material (prominences) can be found along the axes of arcades (Tandberg-Hanssen, 1974). Active region prominences are often cylindrical and show a fine structure in the form of thin filaments, helically twisted around the cylinder axis (Tandberg-Hanssen, 1974; Tandberg-Hanssen and Malville, 1974; Vršnak and Ruždjak, 1982; Vršnak, 1984a, 1985; Vršnak *et al.*, 1988). It is widely accepted that such boundle of cold filaments disclose a pinch-like magnetic field configuration (Anzer and Tandberg-Hanssen, 1970; Kuperus and Van Tend, 1981; Schmieder *et al.*, 1985a, b). Observations indicate that the internal structure of these boundles is approximately equivalent to a uniformly twisted magnetic tube carrying an effective electric current of about some 10^{11} A (Vršnak *et al.*, 1988), which is typical for solar prominences (Ballester and Kleczek, 1984). A similar pinched pattern usually develops from a slab geometry in the pre-eruptive phase or during the eruption of quiescent prominences (Tandberg-Hanssen, 1974).

Observations of the internal structure in prominences immediately before the eruption provide a test for various stability analyses (Sakurai, 1976; Anzer, 1978; Van Tend and Kuperus, 1978; Pneuman, 1980; Priest, 1982; Hood and Anzer, 1987). On the other hand, the development of internal structure during the eruption (House and Berger,

* Paper presented at the 11th European Regional Astronomical Meetings of the IAU on 'New Windows to the Universe', held 3–8 July, 1989, Tenerife, Canary Islands, Spain.

Astrophysics and Space Science **170**: 141–147, 1990.

1987) could be a key for a better comprehension of the dynamics of the process (Pneuman, 1984).

2. Stability of Electric Current Filament

The problem of evolution and stability of an arcade is governed by several physical constraints. The magnetic field lines constituting an arcade, as well as both 'legs' of the magnetic tube associated with the electric current filament are 'anchored' in the photosphere where the convective flows drive electric currents by shearing the arcade and twisting the magnetic tube at its core. Furthermore, the induced eddy current system at the photospheric boundary governs the filament equilibrium. Usually, the problem is treated as two-dimensional, but the curvature of the filament axis introduces extra terms in the equation of motion (Mouschovias and Poland, 1978; Vršnak, 1984). The material in the filament is frequently at chromospheric temperatures with densities up to 10^{11} cm^{-3}, and so the gravitational force must be taken into account. Finally, depending on the strength, the presence of the background field should be considered. It causes a Lorentz force either in upward direction (Kippenhahn–Schlüter-type of prominences) or in downward direction (Kuperus–Raadu-type of prominences).

If we neglect the presence of gas pressure gradients the net force per unit length of the filament in the vertical direction (Vršnak, 1984) can be written as

$$F = F_k - F_t + F_m - F_g \pm F_B \,. \tag{1}$$

The terms F_k and F_t arise when the curvature of the cylinder axis is considered. The Lorentz force caused by the induced photospheric currents is denoted as F_m, while F_g

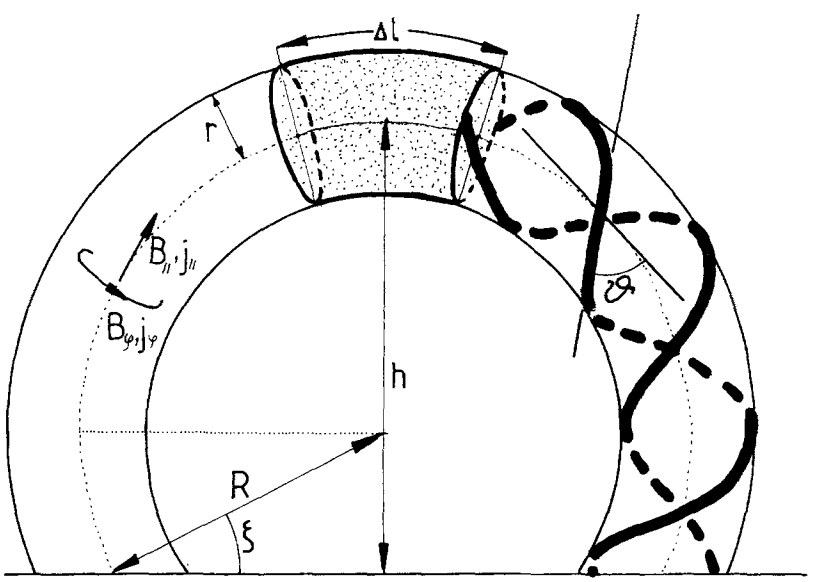

Fig. 1. A helical prominence sketched as a circularly curved cylinder of uniform radius.

and F_B are the gravitational force and the Lorentz force caused by the background field, respectively. The force F_k is caused by the upward, kink-type, magnetic pressure gradient of the azimuthal field B_ϕ, and F_t is the tension of the longitudinal component $B_\parallel$ (Vršnak, 1984).

We will represent the filament as a circularly curved cylinder with a diameter uniform along the axis which is anchored in the photosphere at the footpoint distance $2d$. The cylinder will be characterized by the height of its axis (h) and the corresponding axis length (L) and radius of curvature (R). These parameters can be related to the 'aspect' angle ζ from one of footpoints to the center of circle as $R = d/\cos\zeta$, $h = R + d\,\mathrm{tg}\,\zeta$ and $L = R\pi + 2R\zeta$ (Figure 1). We will describe the internal magnetic field configuration as a slightly curved uniform-twist force-free field with azimuthal and longitudinal components $B_\phi(\rho) = X\rho B/(X^2\rho^2 + 1)$ and $B_\parallel(\rho) = B/(X^2\rho^2 + 1)$, respectively. The magnetic field at the axis of the tube is denoted as B, ρ is the radial distance from the axis normalized with respect to the radius of the tube r and X is the ratio of the components at the edge of the cylinder. The parameter $X = B_\phi/B_\parallel$ is related to the pitch angle of the field lines at $\rho = 1$ (ϑ) as $\mathrm{tg}\,\vartheta = X$.

The terms F_k and F_t for an element of tube of length Δl at its summit can be approximately expressed as

$$F_k = \frac{\mu_0 I^2 \Delta l}{4\pi R}\ ; \qquad F_t = \frac{\mu_0 I^2 \Delta l}{2\pi R X^2}\ , \tag{2}$$

where $I = 2r\pi B_\phi/\mu_0$ is the electric current flowing along the filament. The force F_m on the same element will be approximated by a Lorentz force exerted on a straight wire, carrying current I at height h, by its 'mirror current' (Kuperus and Raadu, 1974):

$$F_m = \frac{\mu_0 I^2 \Delta l}{4\pi h}\ . \tag{3}$$

The gravitational force on the element can be expressed as

$$F_g = gM\Delta l/L\ , \tag{4}$$

where M is the mass of the prominence and g is the acceleration of gravitation at the height h. Here we will consider the case when the last term in Equation (1) $F_B = IB_0 r^2\pi$ can be neglected, due to the small value of the background field B_0.

If we consider the conservation of $B_\parallel$ flux (Ψ), for the assumed internal magnetic field configuration one obtains the relation

$$\Psi = 2\pi r^2 B\,\frac{\ln(X^2+1)}{X^2} = \frac{\mu_0 rI}{Xf(X)} = \text{const.}\ , \tag{5}$$

where $f(X) = X^2/(X^2+1)\ln(X^2+1)$. The approximation that the radius of the cylinder is uniform along the axis means that the pitch of the field lines is also uniform and then the twist can be expressed as $\Phi = LX/r$. Since the field lines are anchored, the

twist is prescribed at the photospheric boundary and Φ = const. during the eruption. If we assume that current I is driven by photospheric convective motions it can be also taken as constant since $\nabla \times \mathbf{B} = \mu_0 \mathbf{j}$ evolves slowly in the photosphere due to its large inertia. Taking also $\Phi = LX/r$ = const., one obtains

$$L/f(X) = \text{const.}\,, \tag{6}$$

which relates X with L, i.e., also with the height h. For $X^2 \gg 1$ and $X_0^2 \gg 1$, Equation (6) can be approximately expressed as $X \approx X_0 L_0/L$ where subscript 0 denotes initial values. The equation of motion for a tube element at its summit (Figure 1) can be finally expressed as:

$$\ddot{h} = A(L/h + L/R - 2L/RX^2) - g\,, \tag{7}$$

where $A = \mu_0 I^2/4\pi M$, and X is determined by Equation (6).

Equation (7) provides several classes of solutions depending on parameters A and X_0 as illustrated by the examples in Figure 2, where we denoted $Z = h/d$. The parameters used for the curve 'a' represent a stable, low-lying prominence, while the curve 'd' represents a stable loop-type prominence. When the prominence is displaced from the equilibrium position a restoring force causes oscillations with periods of about 10–100 min depending on the parameters characterizing the prominence. Such periods

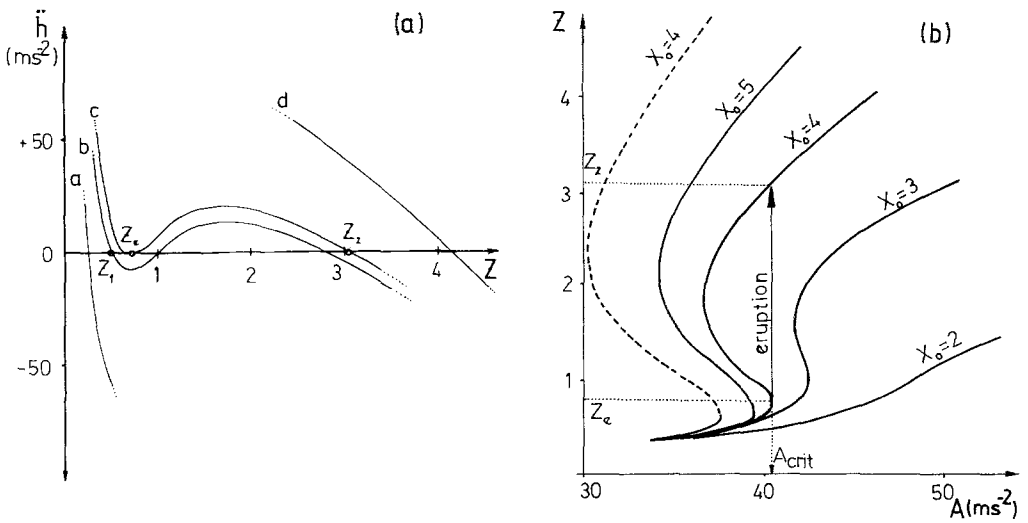

Fig. 2a. The acceleration at the prominence summit as a function of $Z = h/d$ for $d = 60000$ km and $X = 4$ at $Z = 1$. Cases 'a' ($A = 30\ \mathrm{ms}^{-2}$) and 'd' ($A = 50\ \mathrm{ms}^{-2}$) illustrate stable prominences. The case 'b' ($A = 38\ \mathrm{ms}^{-2}$) represents a metastable prominence and the case 'c' ($A = 40.5\ \mathrm{ms}^{-2}$) an unstable prominence. We denoted the lower and upper equilibria as Z_1 and Z_2, and the unstable equilibrium as Z_e.
Fig. 2b. The equilibrium height as a function of the parameter A for $d = 6 \times 10^4$ km (bold lines) and $d = 10^5$ km (broken line). The case $X_0 = 2$ represents a stable prominence which rises through a series of equilibria when A increases. The other examples represent metastable prominences which erupt when A reaches critical value.

are consistent with the observations of prominence oscillations (see Schmieder, 1988, and references therein). A filament described by the curve '*b*' is metastable since for a sufficient displacement it would reach the region where $\ddot{h} > 0$ for $\Delta h > 0$ and would erupt. The curve '*c*' represents an unstable prominence since it erupts for an infinitesimal displacement from the equilibrium position Z_e. A prominence evolves from a metastable state to the instability when the parameter A increases, 'rising' the curve '*b*' up to curve '*c*'.

3. Process of Eruption

In Figure 2(b) we present the dependence of the equilibrium height Z_1 on the parameter A for several values of X at $Z = 1$ (further referred as X_0). If the value of parameter A increases the prominence rises slowly through a series of equilibria until reaching A_{crit} at Z_e, after which no neighbouring equilibrium exists. The prominence erupts from Z_e to a new equilibrium Z_2 (sketched for $X_0 = 4$) and the process is governed by Equation (7). However, when the value of the parameter X_0 is below the critical value, eruption is not possible since Z_e does not exist (sketched for $X_0 = 2$). Such a process was reported by Vršnak and Ruždjak (1982) and Vršnak *et al.* (1988). The evolution of the parameter A can be caused in a number of ways: e.g., A increases if some mass leaks through the legs of the prominence, or if the current I increases due to changes in photospheric magnetic field, usually referred as emerging or merging flux process (Raadu *et al.*, 1987). On the other hand, the change of the parameter A could be neglected during the eruption (Figure 2(b)) since on the short time-scale the change of the photospheric magnetic field (and so the change of I) can be neglected due to inertia of photosphere.

In Figure 3(a) we present some of the results based on the observations of the eruptive prominence of 16 August, 1988 (the detailed description will be given in separate paper). The observations expose a typical behaviour for an eruptive prominence: after a slow rise the acceleration started ($t > 44$ min) and was followed by a deceleration ($t > 140$ min) after a phase characterized by a constant ascending velocity. The pitch of helical streamers was measured close to the prominence summit at several moments and it was decreasing (Figure 3(b)). The measured dependence $h(t)$ was fitted by the 4th-degree polynomial (Figure 3(a)) and from it we found the acceleration $\ddot{h}_{\text{obs}}(t)$ presented in Figure 3(a). In Figure 3(b) the curve $\ddot{h}_{\text{calc}}(Z)$ is based on Equation (7) and the parameters inferred from the observations ($d = 60\,000$ km; $X_0 = 4$). The correspondence between the observations and the model is good at the beginning of the process. To describe properly the end of the process, i.e., the deceleration phase, a 'coronal friction' (Hyder, 1966) must be taken into account. The observations of the oscillating prominences (Ramsey and Smith, 1966; Kleczek and Kuperus, 1969; Vršnak, 1984) disclosed considerable 'friction' causing a damping of the oscillations characterized by the decay $\delta \approx 10^{-3}\ \text{s}^{-1}$. Such 'friction' can cause a considerable reduction of acceleration of an eruptive prominence. Furthermore, comparing the value of δ with the calculated frequency of free oscillations at the upper equilibrium point Z_2,

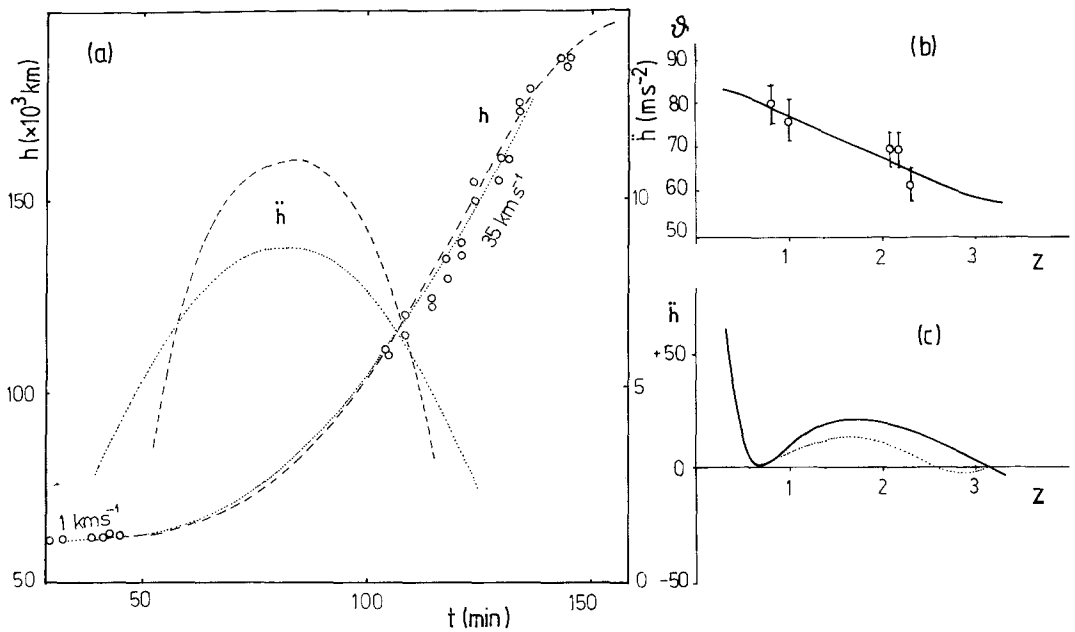

Fig. 3a. The height (h) as a function of time (t) for the eruptive prominence of 16 August, 1988. The 4th degree polynomial least-square fit is presented by dotted line, and 4th-degree polynomial fixed by $\ddot{h} = 0$ at $t = 44$ min and $t = 120$ min by broken line. The inferred acceleration is denoted as $\ddot{h}$.

Fig. 3b. The calculated pitch angle $\vartheta(Z)$. The measured pitch angles are indicated together with the error bars.

Fig. 3c. The calculated dependence $\ddot{h}(Z)$ (bold line) and the qualitative behaviour of $\ddot{h}$, when the 'coronal friction' is taken into account (dotted line).

which amounts to about $\omega_0 = 5 \times 10^{-4}$ rad s^{-1} in this case, one finds $\delta > \omega_0$. Since $\delta > \omega_0$, the prominence will monotonically approach Z_2 instead of oscillating; so the highest point reached by the prominence is Z_2. The observations give $Z_{\max} = 3.3$ which is consistent with the value of Z_2 determined from Figure 3.

4. Discussion and Conclusion

The proposed model for an arcade eruption is based on the structure of the electric current filament at its core. A simple consideration of the forces appearing in cylindrical prominences relates a stable low-lying prominences with metastable prominences and loop-prominences. It explains prominence and loop oscillations and predicts the criteria and scenario for the eruptive instability onset. The phase of slow rise through series of equilibrium states, caused either by mass loss or by increase of longitudinal electric current ($\Delta A > 0$), leads metastable prominence to the eruptive instability which results in upward acceleration and 'detwisting'. At the end of the acceleration process the coronal 'friction' plays an important role and the prominence stops at the upper equilibrium position. The basic features are common for most of the eruptive promi-

nences. In the case of the prominence of 16 August, 1988 where the changes of internal structure were followed, the model is in good agreement with the observations. For the values of the twist below the critical value the eruption can not occur and the prominence evolves quasistatically as observed in the case described by Vršnak and Ruždjak (1982).

References

Anzer, U.: 1978, *Solar Phys.* **57**, 111.
Anzer, U. and Tandberg-Hanssen, E.: 1970, *Solar Phys.* **11**, 61.
Ballester, J. L. and Kleczek, J.: 1984, *Solar Phys.* **90**, 37.
Hood, A.: 1988, in J. L. Ballester and E. R. Priest (eds.), *Dynamics and Structure of Solar Prominences*, Palma de Mallorca, 1987, Universitas de les Illes Balears, p. 147.
Hood, A. and Anzer, U.: 1987, *Solar Phys.* **111**, 333.
House, L. L. and Berger, M. A.: 1987, *Astrophys. J.* **323**, 406.
Hyder, A. W.: 1966, *Z. Astrophys.* **63**, 78.
Kleczek, J. and Kuperus, M.: 1969, *Solar Phys.* **6**, 72.
Kuperus, M. and Raadu, M. A.: 1974, *Astron. Astrophys.* **31**, 189.
Kuperus, M. and Van Tend, W.: 1981, *Solar Phys.* **71**, 125.
Mouschovias, T. Ch. and Poland, A. I.: 1978, *Astrophys. J.* **220**, 675.
Pneuman, G. W.: 1980, *Solar Phys.* **65**, 369.
Pneuman, G. W.: 1984, *Solar Phys.* **94**, 299.
Priest, E. R.: 1982, *Solar Magnetohydrodynamics*, D. Reidel Publ. Co., Dordrecht, Holland.
Raadu, M. A., Schmieder, B., Mein, N., and Gesztely, L.: 1987, *Hvar Obs. Bull.* **11**, 105.
Ramsey, H. E. and Smith, S. F.: 1966, *Astron. J.* **71**, 197.
Sakurai, T.: 1976, *Publ. Astron. Soc. Japan* **28**, 177.
Schmieder, B.: 1988, in J. L. Ballester and E. R. Priest (eds.), *Dynamics and Structure of Solar Prominences*, Palma de Mallorca, 1987, Universitas de les Illes Balears, p. 17.
Schmieder, B., Raadu, M. A., and Malherbe, J. M.: 1985a, *Astron. Astrophys.* **142**, 249.
Schmieder, B., Malherbe, J. M., Poland, A. I., and Simon, G.: 1985b, *Astron. Astrophys.* **153**, 64.
Sheeley, N. R., Jr., Bohlin, J. D., Brueckener, G. E., Purcell, J. D., Scherrer, V., and Tousey, R.: 1975, *Solar Phys.* **40**, 103.
Švestka, Z.: 1989, in M. Vazquez (ed.), *New Windows to the Universe,* Cambridge Univ. Press, Cambridge.
Tandberg-Hanssen, E.: 1974, *Solar Prominences*, D. Reidel Publ. Co., Dordrecht, Holland.
Tandberg-Hanssen, E. and Malville, J. M.: 1974, *Solar Phys.* **39**, 107.
Van Tend, W. and Kuperus, M.: 1978, *Solar Phys.* **59**, 115.
Vršnak, B.: 1984a, *Hvar Obs. Bull.* **8**, 13.
Vršnak, B.: 1984b, *Solar Phys.* **94**, 289.
Vršnak, B.: 1985, *Hvar Obs. Bull.* **9**, 61.
Vršnak, B. and Ruždjak, V.: 1982, *Hvar Obs. Bull.* **6**, 123.
Vršnak, B., Ruždjak, V., Brajša, R., and Džubur, A.: 1988, *Solar Phys.* **116**, 45.